available at www.sciencedirect.com

ScienceDirect

journal homepage: www.elsevier.com/locate/biochempharm

# Inhibition of the HERG potassium channel by the tricyclic antidepressant doxepin

R.S. Duncan [a], M.J. McPate [a], J.M. Ridley [a], Z. Gao [a], A.F. James [a], D.J. Leishman [b,c], J.L. Leaney [b], H.J. Witchel [a,*], J.C. Hancox [a,*]

[a] Department of Physiology and Cardiovascular Research Laboratories, School of Medical Sciences, University Walk, Bristol, BS8 1TD, UK
[b] Pfizer Global Research & Development, Sandwich Laboratories, Ramsgate Road, Sandwich, Kent CT13 9NJ, UK
[c] Lilly Research Laboratories, Greenfield Laboratories, PO Box 708, Greenfield IN, 46140, USA

ARTICLE INFO

*Article history:*
Received 14 January 2007
Accepted 27 April 2007

*Keywords:*
Antidepressant
Arrhythmia
Doxepin
HERG
$I_{Kr}$
Long QT syndrome
Potassium channel
QT interval
QT-prolongation
Rapid delayed rectifier
Short QT syndrome
*Torsade de pointes*

ABSTRACT

HERG (human ether-à-go-go-related gene) encodes channels responsible for the cardiac rapid delayed rectifier potassium current, $I_{Kr}$. This study investigated the effects on HERG channels of doxepin, a tricyclic antidepressant linked to QT interval prolongation and cardiac arrhythmia. Whole-cell patch-clamp recordings were made at 37 °C of recombinant HERG channel current ($I_{HERG}$), and of native $I_{Kr}$ 'tails' from rabbit ventricular myocytes. Doxepin inhibited $I_{HERG}$ with an $IC_{50}$ value of 6.5 ± 1.4 μM and native $I_{Kr}$ with an $IC_{50}$ of 4.4 ± 0.6 μM. The inhibitory effect on $I_{HERG}$ developed rapidly upon membrane depolarization, but with no significant dependence on voltage and with little alteration to the voltage-dependent kinetics of $I_{HERG}$. Neither the S631A nor N588K inactivation-attenuating mutations (of residues located in the channel pore and external S5-Pore linker, respectively) significantly reduced the potency of inhibition. The S6 point mutation Y652A increased the $IC_{50}$ for $I_{HERG}$ blockade by ~4.2-fold; the F656A mutant also attenuated doxepin's action at some concentrations. HERG channel blockade is likely to underpin reported cases of QT interval prolongation with doxepin. Notably, this study also establishes doxepin as an effective inhibitor of mutant (N588K) HERG channels responsible for variant 1 of the short QT syndrome.



## 1. Introduction

Diverse cardiac and non-cardiac drugs are associated with prolongation of the rate-corrected QT ($QT_c$) interval of the electrocardiogram and with a risk of the potentially fatal arrhythmia *Torsade de Pointes* (TdP) [1–4]. The majority of such agents exert a common action of inhibiting the cardiac rapidly activating delayed rectifier $K^+$ current ($I_{Kr}$). $I_{Kr}$ is a major determinant of ventricular action potential repolarization and, thereby, of the $QT_c$ interval [2,4,5]. The pore-forming subunit of $I_{Kr}$ channels is encoded by HERG (human ether-à-go-go-related gene [6,7]). HERG channels appear to have a larger pore cavity than other (Kv) six transmembrane domain $K^+$ channels and possess particular aromatic amino-acid residues in the S6 region of the channel [5,8–10]. These features combine to confer a high susceptibility to pharmacological blockade upon the HERG channel. Indeed, the association between drug-induced $QT_c$ interval prolongation and pharmacological blockade of HERG channels is sufficiently strong that drug-screening against recombinant HERG channels is now an important component of cardiac safety-pharmacology during drug development [11–13].

* *Corresponding authors*. Tel.: +117 928 9028; fax: +117 928 8923.
E-mail addresses: harry.witchel@bristol.ac.uk (H.J. Witchel), jules.hancox@bristol.ac.uk (J.C. Hancox).
0006-2952/$ – see front matter 
doi:10.1016/j.bcp.2007.04.024

Doxepin is a tricyclic antidepressant (TCA) structurally related to amitriptyline and imipramine that combines antidepressant and sedative actions [14]. Initially doxepin was suggested to have better cardiac safety than other TCA drugs [15]. However, a subsequent review of the clinical and animal data [16] and a study in depressed patients [17] found no evidence that doxepin had fewer cardiovascular effects than other TCAs. Moreover, similar to other TCAs, doxepin can be cardiotoxic in overdose [14]. Adverse cardiac effects associated with doxepin include premature ventricular complexes (PVCs) and wide QRS complexes on the electrocardiogram. Furthermore, there are a number of documented cases of QT interval prolongation with doxepin [18–20]. For example, in overdose doxepin has been associated with a greatly prolonged $QT_c$ interval (reaching 580 ms) and TdP [19], whilst QT interval prolongation and syncope have been reported for doxepin in combination with methadone and β blocker use [20]. At present there is no information on the basis for $QT_c$ prolongation with doxepin. However, other TCAs including imipramine and amitryptiline have been demonstrated to inhibit recombinant HERG channels [21–23] and we hypothesised that doxepin is also likely to act as an inhibitor of HERG channel current ($I_{HERG}$). The present study was conducted to test this hypothesis and to characterise the nature of any observed $I_{HERG}$ blockade.

## 2. Methods

### 2.1. *Maintenance of mammalian cell lines stably expressing wild-type and mutant HERG channels*

Experiments on wild-type HERG were performed on a cell line (Human Embryonic Kidney; HEK 293) stably expressing HERG (donated by Dr Craig January, University of Wisconsin [24]), except for those in Fig. 8; these utilised a cell line stably expressing lower levels of HERG developed in this laboratory, for use with high external $[K^+]$ (for comparison with the F656A mutant, see Section 2.2 below). Cell lines stably expressing HERG and its mutants, F656A and Y652A were maintained as described previously [25]. Cell lines stably expressing the S631A [26] and N588K [27] mutants were made from appropriately mutated HERG sequences using previously described methods [25]. Cells were passed using a non-enzymatic dissociating agent (Splitase, AutogenBioclear) and plated out onto small sterilised glass coverslips in 30 mm petri dishes containing a modification of Dulbecco's modified Eagle's medium with Glutamax-1 (DMEM; Gibco, Gibco/Invitrogen, Paisley, UK), supplemented with 10% fetal bovine serum (Gibco), 400 $\mu g\,ml^{-1}$ gentamycin (Gibco) and 400 $\mu g\,ml^{-1}$ geneticin (G418; Gibco). Treatment of the mutant cell lines was identical to treatment of the wild-type cell line except that cultures were maintained with 800 $\mu g\,ml^{-1}$ of hygromycin. The cells were incubated at 37 °C for a minimum of two days prior to any electrophysiological study.

### 2.2. *Experimental solutions*

Whole-cell patch-clamp measurements of wild-type (WT) and mutant $I_{HERG}$ were made at 37 ± 1 °C. Once in the experimental chamber cells were superfused with a standard extracellular Tyrode's solution containing (in mM): 140 NaCl, 4 KCl, 2.5 $CaCl_2$, 1 $MgCl_2$, 10 glucose, 5 HEPES, (titrated to pH 7.45 with NaOH). Similar to other studies from our laboratory (e.g. [28,29]), for experiments employing the S6 mutant F656A (which shows comparatively low levels of channel expression [8,25]) and its WT control, the external solution contained 94 mM KCl (the NaCl concentration was correspondingly reduced). Experimental solutions were applied using a home-built, warmed, solution delivery system that exchanged the solution surrounding a cell in <1 s. Doxepin powder (Sequoia Research Products and Sigma-Aldrich) was dissolved in Tyrode's solution to produce initial stock solutions of either 10 or 50 mM, which were serially diluted to produce working solutions ranging from 0.1 μM to 1 mM.

The pipette dialysis solution for $I_{HERG}$ measurement contained (in mM): 130 KCl, 1 $MgCl_2$, 5 EGTA, 5 MgATP, 10 HEPES (titrated to pH 7.2 with KOH) [28,29]. Patch-pipettes were heat-polished to 2.5–4 MΩ. No correction was made for the 'pipette-to-bath' liquid junction potential, which was measured to be −3.2 mV.

### 2.3. *Experiments on rabbit isolated ventricular myocytes*

One series of experiments was performed to investigate blockade by doxepin of native $I_{Kr}$ from adult ventricular myocytes (Results, Fig. 2). For these, male New Zealand white rabbits (2–3 kg) were killed humanely in accordance with UK Home Office legislation. Ventricular myocytes were then isolated by a combination of mechanical and enzymatic dispersion, using previously described methods [30,31]. Pipette and external solutions for $I_{Kr}$ measurement were identical to those described above for $I_{HERG}$ measurement.

### 2.4. *Electrophysiological recording and analysis*

Whole-cell patch-clamp recordings were made using Axopatch 200 or 200B amplifiers (Axon Instruments) and a CV201 head-stage. Between 75 and 80% of the pipette series resistance was compensated. Voltage-clamp commands were generated using 'WinWCP' (John Dempster, Strathclyde University), Clampex 8 (Axon Instruments), or 'Pulse' software (HEKA Electronik). Data were recorded either via a Digidata 1200B interface (Axon Instruments) or an Instrutech VR-10B interface and stored on the hard-disk of a personal computer. The voltage-protocols employed for specific experiments are described either in the relevant 'results' text, or are shown diagrammatically on the relevant figures; unless otherwise stated in the text, the holding membrane potential between experimental sweeps was −80 mV. Data are presented as mean ± S.E.M. Statistical comparisons were made using, as appropriate, paired and unpaired t-tests or one-way analysis of variance (Anova) (Prism 3 or Instat, Graphpad Inc.). $P$ values of less than 0.05 were taken as significant; ns = no statistically significant difference.

The following equations were used for numerical analysis and graphical fits to data:

The extent of $I_{HERG}$ inhibition by differing concentrations of doxepin was determined using the equation:

$$\text{Fractional block} = 1 - \left(\frac{I_{HERG-DOXEPIN}}{I_{HERG-CONTROL}}\right) \quad (1)$$

where 'Fractional block' refers to the degree of inhibition of $I_{HERG}$ by a given concentration of doxepin; $I_{HERG-DOXEPIN}$ and $I_{HERG-CONTROL}$ represent current amplitudes in the presence and absence of doxepin.

Concentration–response data were fitted by a standard Hill equation of the form:

$$\text{Fractional block} = \frac{1}{1 + (IC_{50}/\text{DOXEPIN})^h} \quad (2)$$

where $IC_{50}$ is [DOXEPIN] producing half-maximal inhibition of the $I_{HERG}$ tail and $h$ is the Hill coefficient for the fit.

Half-maximal voltage values for $I_{HERG}$ activation were obtained by fitting $I_{HERG}$ tail-voltage ($I$–$V$) relations with a Boltzmann distribution equation of the form:

$$I = \frac{I_{max}}{(1 + \exp(\frac{V_{0.5} - V_m}{k}))} \quad (3)$$

where $I$ is the $I_{HERG}$ tail amplitude following test potential $V_m$, $I_{max}$ the maximal $I_{HERG}$ tail observed during the protocol, $V_{0.5}$ the potential at which $I_{HERG}$ was maximally activated, and $k$ is the slope factor describing $I_{HERG}$ activation. Data from each individual experiment were fitted by this equation to derive $V_{0.5}$ and $k$ values in 'control' and with doxepin. The resultant mean $V_{0.5}$ and $k$ values obtained from pooling values from each experiment were then used to calculate the mean activation relations plotted in Fig. 3.

Parameters describing voltage-dependent inactivation of $I_{HERG}$ were derived from fits to voltage-dependent availability plots with the equation:

$$\text{Inactivation parameter} = 1 - \left(\frac{1}{(1 + \exp((V_{0.5} - V_m)/k))}\right) \quad (4)$$

where 'inactivation parameter' at any test potential, $V_m$, occurs within the range 1–0, $V_{0.5}$ is the voltage at which $I_{HERG}$ was half-maximally inactivated and $k$ describes the slope factor for the relationship.

## 3. Results

### 3.1. Doxepin produces concentration-dependent inhibition of WT $I_{HERG}$

$I_{HERG}$ was elicited by the protocol shown in the inset of Fig. 1A, which is a standard protocol used to study $I_{HERG}$ pharmacology in this laboratory (e.g. [28,29,32]). Membrane potential was stepped from −80 to +20 mV for 2 s followed by a 4-s step to −40 mV to elicit $I_{HERG}$ tails. A brief (50 ms) pulse to −40 mV preceded the step to +20 mV in order to monitor the instantaneous current without activation of $I_{HERG}$ (peak outward $I_{HERG}$ tails on repolarization to –40 mV were compared with the instantaneous current during the 50 ms pulse to −40 mV, in order to measure $I_{HERG}$ tail amplitude). This voltage protocol was applied repeatedly (at 20 s intervals) prior to and during the application of doxepin. Fig. 1A shows a representative recording of $I_{HERG}$ in control, 5 min after the addition of 10 μM doxepin and 5 min following wash-out of the drug. Doxepin produced a substantial inhibition of $I_{HERG}$; this was largely reversible upon washout (to 73 ± 9% of control in six cells to which 10 μM doxepin was applied). Fig. 1B shows records for the same cell before and at increasing times during doxepin exposure, indicating that blockade was maximal within 4–5 min of drug application. Fig. 1C shows a plot of mean ± S.E.M. fractional block of $I_{HERG}$ tails by four different concentrations of doxepin, fitted by Eq. (2). The $IC_{50}$ for doxepin inhibition of $I_{HERG}$ with this protocol was 6.5 ± 1.4 μM and the Hill coefficient for the fit was 1.0 ± 0.2. $I_{HERG}$ blockade by doxepin was not accompanied by statistically significant changes to the time-course of deactivation of the time-dependent component of $I_{HERG}$ tails on repolarization to −40 mV: bi-exponential fitting of the time-dependent tail current decline yielded fast time-constants of deactivation ($\tau_{fast}$) of 203 ± 15 and 273 ± 21 ms in control solution and 10 μM doxepin, respectively ($n = 6$; $p > 0.05$, paired t-test), and slow time-constants of deactivation ($\tau_{slow}$) of 1164 ± 141 and 1499 ± 131 ms ($p > 0.1$). Doxepin did not influence significantly the relative proportions of deactivating current described by the fast and slow time-constants of deactivation (the proportion of deactivating current fitted by the $\tau_{fast}$ was ~0.6 in both control and doxepin).

It has been suggested that pharmacological inhibition of $I_{HERG}$ by some drugs may vary between different stimulus protocols [33]. Therefore, we also investigated $I_{HERG}$ blockade by doxepin using an action potential (AP) voltage waveform [32,34]. The voltage-command used (shown in the lower panel of Fig. 2A) was a previously acquired, digitised AP from a rabbit ventricular myocyte. This was applied repeatedly (at 4 s intervals) from a holding potential of −80 mV [32]. The upper panel of Fig. 2A shows traces in the absence and presence of doxepin. Peak outward $I_{HERG}$ during the repolarizing phase of the AP was inhibited 60 ± 12% ($n = 5$) by 10 μM doxepin, which does not differ significantly from the extent of $I_{HERG}$ tail current blockade by this concentration obtained using the protocol shown in Fig. 1 (62 ± 4%; $n = 6$; $p > 0.8$; unpaired t-test).

In order to determine effects of doxepin on native $I_{Kr}$, three drug concentrations (1, 10 and 100 μM) were applied to ventricular myocytes under whole-cell patch clamp. The command protocol for these experiments (similar to [32]) is shown in Fig. 2B and $I_{Kr}$ tails were monitored on repolarization from +20 to −40 mV. Under our conditions, the outward tail currents observed on repolarization to −40 mV were almost completely abolished by 1 μM dofetilide (91 ± 3% blockade; $n = 7$), verifying that these were carried by $I_{Kr}$ with little or no contamination from overlapping currents. Fig. 2C shows representative $I_{Kr}$ tails on repolarization from +20 to −40 mV in the absence and presence of 100 μM doxepin; at this concentration the current was largely abolished. Fig. 2D contains mean ± S.E.M fractional block data for the tested doxepin concentrations, fitted by Eq. (2). The derived $IC_{50}$ for doxepin inhibition of native $I_{Kr}$ tails was 4.4 ± 0.6 μM, in good

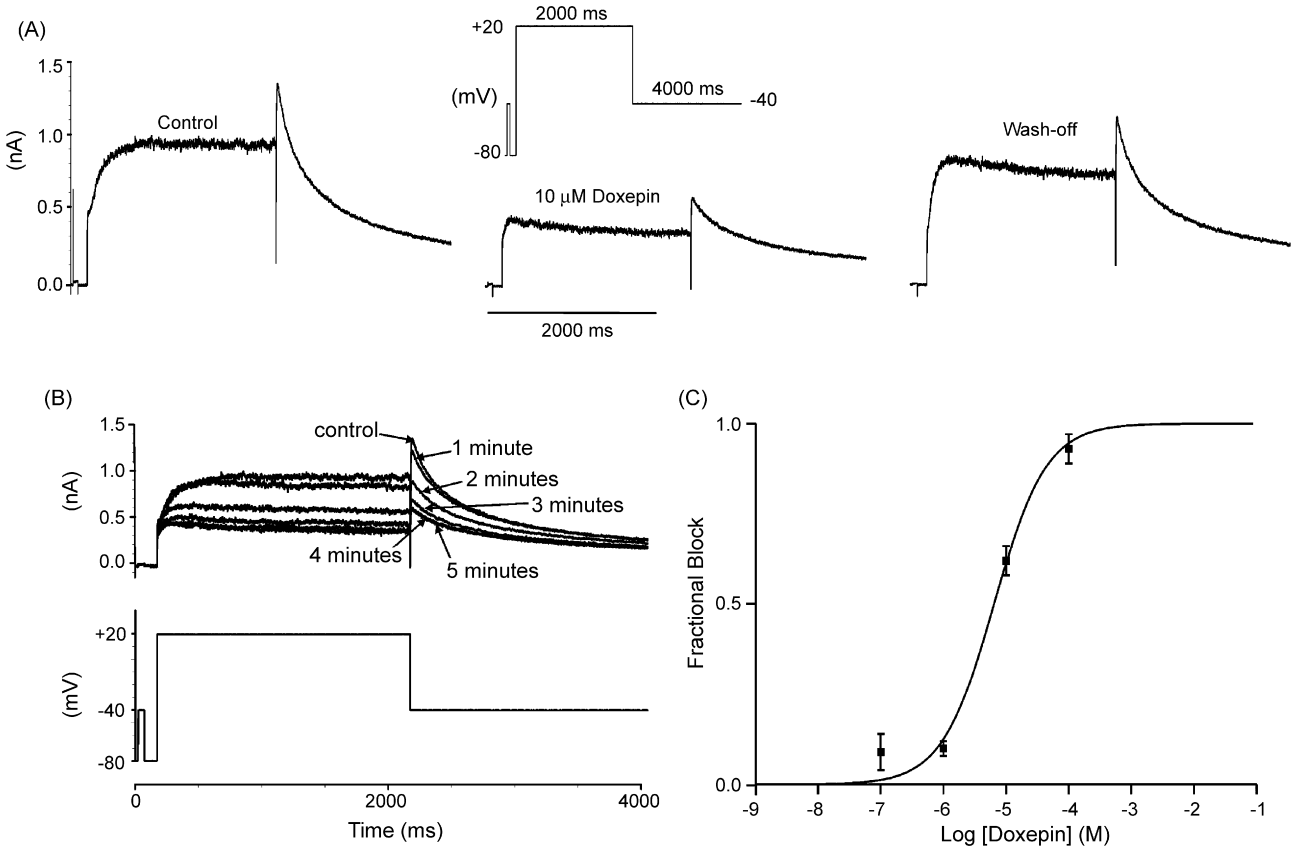


**Fig. 1 – Concentration dependent inhibition of $I_{HERG}$ by doxepin. (A) Representative currents in the absence, presence (5 min) and following wash off (5 min) of 10 μM doxepin, elicited by the voltage protocol shown in the inset. (B) Representative currents (upper traces; lower trace shows voltage protocol), from the same cell as in A, in the absence and during doxepin exposure. 'Control' refers to current prior to doxepin exposure, whilst numbered time-points indicate currents sampled at 1–5 min of doxepin application. (C) Mean fractional block produced by four different concentrations of doxepin fitted with Eq. (2), which yielded an $IC_{50}$ value of 6.5 μM (± 1.4 μM) with a Hill coefficient of 1.0 (± 0.2). Each drug concentration was applied to a minimum of five cells.**

agreement with the observed inhibitory potency of doxepin on $I_{HERG}$.

### 3.2. *Voltage dependence of $I_{HERG}$ blockade by doxepin*

Voltage dependence of $I_{HERG}$ blockade by doxepin was determined by the application, in control and doxepin-containing solutions, of a series of 2 s duration depolarizing commands to a range of test potentials up to +40 mV [32]. Successive command pulses were applied at 20 s intervals. Representative control currents at selected command voltages are shown in Fig. 3Ai; currents from the same cell following equilibration in 10 μM doxepin are shown in Fig. 3Aii (upper traces; lower traces in each panel show corresponding voltage commands). At all test potentials, $I_{HERG}$ was inhibited by doxepin. For each of five similar experiments, fractional inhibition of $I_{HERG}$ tails following each voltage command was calculated using Eq. (1); the mean ± S.E.M. fractional block of $I_{HERG}$ tails is plotted against command voltage in Fig. 3B. Also shown in Fig. 3B are voltage-dependent activation relations for $I_{HERG}$ in control solution and in the presence of doxepin (see Section 2). The derived mean $V_{0.5}$ and $k$ values were: control $V_{0.5} = -21.0 \pm 3.1$; doxepin $V_{0.5} = -24.0 \pm 2.2$, $p > 0.1$; control $k = 5.9 \pm 0.2$; doxepin $k = 7.5 \pm 1.7$, $p > 0.3$, with the $I_{HERG}$ activation relations in control and doxepin closely overlying one another (Fig. 3B). Fractional block of $I_{HERG}$ showed no statistically significant dependence on voltage over the range from −40 to + 40 mV ($p > 0.2$; Anova).

The voltage dependence of $I_{HERG}$ availability/inactivation was assessed using a 3-step protocol similar to those used in previous $I_{HERG}$ investigations from our laboratory ([32,35], and shown schematically as an inset to Fig. 3C). Mean data from five experiments were corrected for deactivation [35] and the resulting values were plotted to give availability plots in the absence and presence of doxepin (Fig. 3C); the data-sets were fitted with Eq. (4) (see Section 2). In control and doxepin the inactivation $V_{0.5}$ values were, respectively, $-37.9 \pm 2.4$ and $-43.5 \pm 4.1$ mV (ns, paired t-test), with corresponding $k$ values of $-16.2 \pm 2.4$ and $-17.3 \pm 8.8$ mV (ns, paired t-test). Thus, doxepin did not alter the voltage-dependence of $I_{HERG}$ inactivation. Although there was a trend towards an acceleration in the time-course of $I_{HERG}$ inactivation, this did not attain statistical significance (inactivation time–constant of $3.3 \pm 1.2$ ms in control versus $1.4 \pm 0.6$ ms in doxepin, $p > 0.1$;

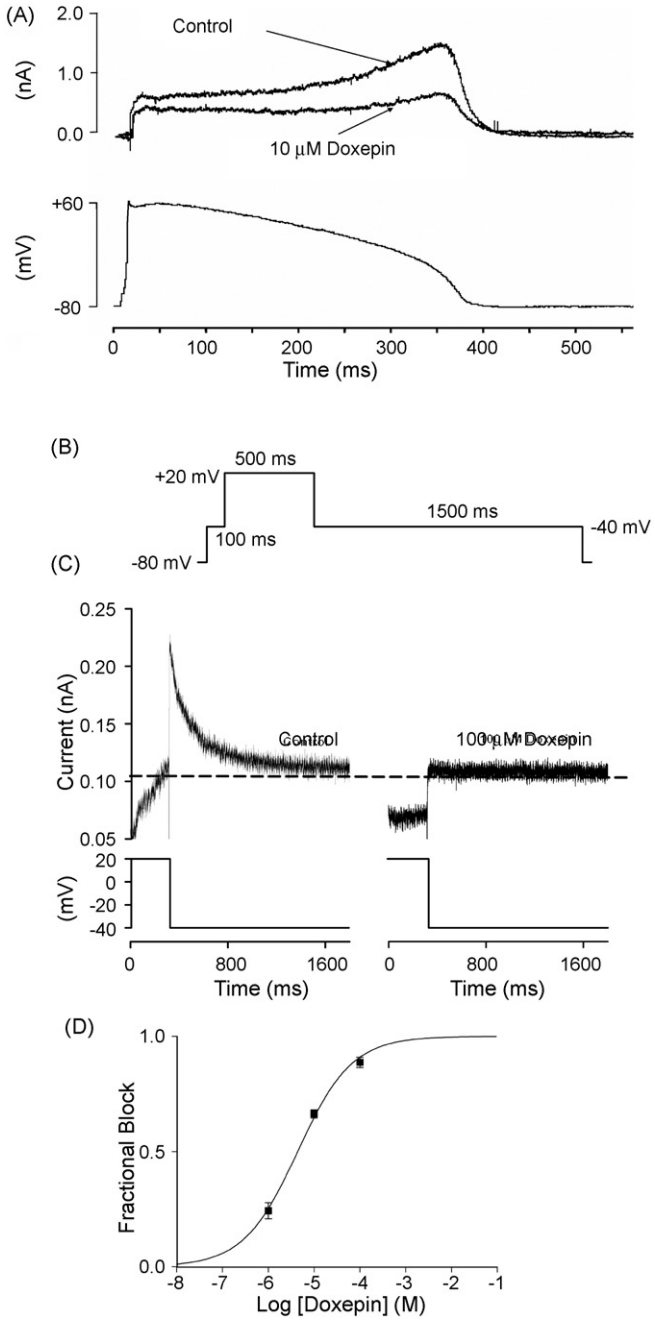


**Fig. 2 – Doxepin inhibition of $I_{HERG}$ during action potential (AP) voltage clamp and of native $I_{Kr}$ tails. (A) The upper traces show (leak corrected) representative currents of heterologously expressed $I_{HERG}$ in the absence and presence of 10 μM doxepin elicited by an AP clamp protocol (lower trace; voltage command applied at 4 s intervals). (B) Schematic representation of protocol used to assess blockade of native $I_{Kr}$ tails by doxepin. (C) Representative tail currents from a rabbit ventricular myocyte upon repolarization from +20 to −40 mV in the absence (left panel) and in the presence of 100 μM doxepin (right panel). Upper traces show current records and lower traces show corresponding portion of the voltage protocol. The horizontal dashed line is drawn at the level of the current at −40 mV at the end of the initial (100 ms) step to −40 mV, against which peak $I_{Kr}$ amplitude on repolarization from +20 to +40 mV was measured. (D) Mean fractional tail current block produced by three different concentrations of doxepin fitted with Eq. (2), which yielded an $IC_{50}$ value of 4.4 (± 0.6 μM) with a Hill coefficient of 0.7 (± 0.1). Each drug concentration was applied to a minimum of twelve cells.**

obtained from exponential fits to the inactivating phase of the current elicited during the third step of the protocol, following a brief hyperpolarizing step to −80 mV).

### 3.3. *Time dependence of $I_{HERG}$ inhibition by doxepin*

Gating-dependence of $I_{HERG}$ inhibition by doxepin was investigated further by the use of two protocols to examine the time-dependence of development of $I_{HERG}$ blockade. The first protocol used a sustained (10 s) depolarizing step to 0 mV from a holding potential of −80 mV (shown in Fig. 4A). This protocol was applied first in the absence of doxepin to elicit control $I_{HERG}$. It was then discontinued whilst cells were equilibrated in 10 μM doxepin (for 7 min), after which it was re-applied. The first current trace recorded on resumption of stimulation was used to determine development of fractional blockade throughout the applied depolarization. Fig. 4A shows representative traces in control and doxepin; these traces diverged rapidly following depolarization, suggesting that $I_{HERG}$ blockade developed rapidly with time. Fig. 4B shows plots of mean ± S.E.M. fractional block of $I_{HERG}$ at various time intervals throughout the applied depolarization (main panel; $n = 8$) and on an expanded time-scale to show development of blockade over the first 0.5 s (inset). These plots show clearly that $I_{HERG}$ blockade developed rapidly on depolarization, with little change in blockade after 200–300 ms following the onset of the voltage-command. The time-course of development of blockade was well-described by a mono-exponential fit to the data, with a rate constant ($K$) for the fit of 16.33 $s^{-1}$ (equivalent to a time-constant ($1/K$) of 61 ms).

Although the protocol used in Fig. 4 is well suited for examining the development of $I_{HERG}$ inhibition over a period of seconds following membrane depolarization, it is less well suited for accurate assessment of blockade of $I_{HERG}$ immediately following membrane depolarization than are protocols based on tail current measurements [29,32]. Therefore, a second protocol was also used [29]. Membrane potential was held at –100 mV and, from this, 10 and 200 ms duration depolarizations to +40 mV were applied, each followed by a period at −40 mV to monitor $I_{HERG}$ tails [29]. Fig. 5A shows representative currents from the same cell activated by 10 ms (Fig. 5Ai) and 200 ms (Fig. 5Aii) commands in the absence and presence of doxepin. Some $I_{HERG}$ tail inhibition was evident following the 10 ms duration command, with further blockade evident after the 200 ms command. Fig. 5B shows mean fractional block of $I_{HERG}$ tails for five similar experiments. Whilst blockade for 200 ms commands was significantly greater than that for 10 ms commands ($p < 0.02$), the occurrence of some blockade with only a very brief duration depolarizing command is concordant with either a very rapidly developing gating-dependent blockade on depolarization or with a contribution of closed-channel block to the overall effect of doxepin [25,29,36].

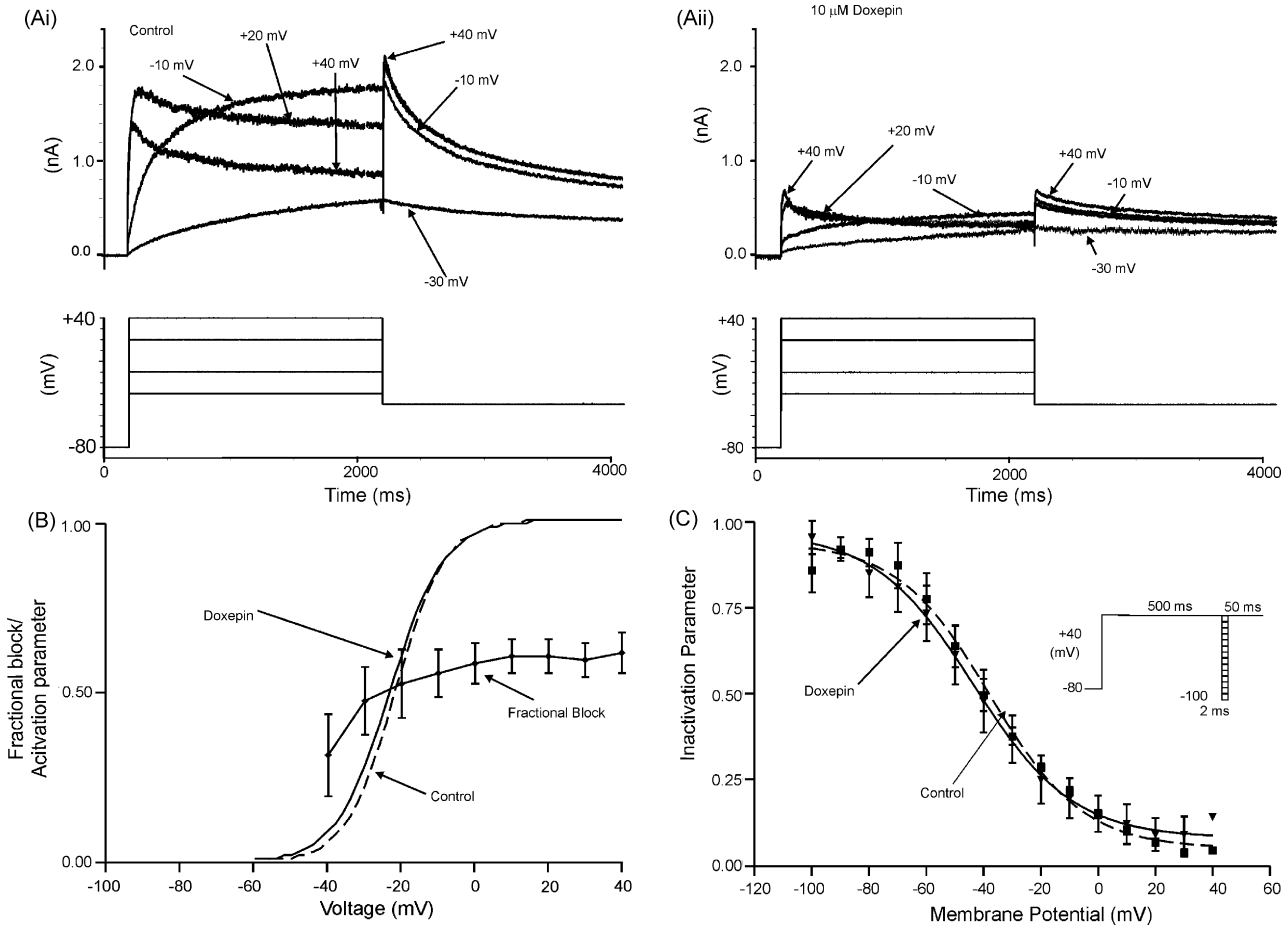


**Fig. 3 – Voltage dependence of $I_{HERG}$ inhibition by doxepin. (A) Representative currents (upper traces) at selected voltages in: (Ai) the absence and (Aii) presence of 10 μM doxepin, elicited by the voltage-protocol shown in the lower traces (only some steps shown, for purposes of clarity of display). (B) Mean fractional block ($n$ = 5) of peak $I_{HERG}$ tails produced by 10 μM doxepin, between test potentials of −40 and +40 mV. Superimposed are the continuous plots of activation curves for $I_{HERG}$ in the absence (dashed line) and presence (continuous line) of doxepin, calculated as described in Section 2. The mean activation $V_{0.5}$ and $k$ values obtained from $I_{HERG}$ tail-voltage relations using Eq. (3) are given in Section 3. (C) Voltage-dependence of $I_{HERG}$ availability/inactivation (protocol shown in inset). The mean ($n$ = 5) normalised data ($I/I_{max}$) were plotted against the test potential and fitted with Eq. (4). The derived half-maximal inactivation values were: control $V_{0.5}$ = −37.9 ± 2.4 mV and doxepin $V_{0.5}$ = − 43.5 ± 4.1 mV in the absence (filled squares, dashed line) and presence (filled triangles, continuous line) of 10 μM doxepin, respectively (ns paired t-test $p$ = 0.79), with corresponding $k$ values of −16.2 ± 2.4 and −17.3 ± 8.8 mV (ns paired t-test $p$ = 0.59).**

### 3.4. *Effect of inactivation-attenuating mutants on $I_{HERG}$ inhibition by doxepin*

In order to investigate further the gating-dependence of $I_{HERG}$ blockade by doxepin, experiments were performed using two inactivation-attenuating HERG mutants: S631A and N588K. Residue S631 is located towards the outer mouth of the HERG channel pore, and the S631A (serine → alanine) mutation has been reported to shift $I_{HERG}$ inactivation by ∼+100 mV [26]. Residue N588 is located in the external S5-Pore linker of the channel, and the N588K (asparagine → lysine) mutation, which is responsible for one form of the recently identified genetic short QT syndrome [27], has been reported to shift $I_{HERG}$ inactivation by ∼+60 to +100 mV [35,37]. The effect of each mutation on the potency of $I_{HERG}$ blockade by doxepin was determined using the same protocol as was used to establish concentration-dependence of WT $I_{HERG}$ blockade (Fig. 1). Fig. 6Ai shows representative currents in control and 10 μM doxepin for WT–HERG, whilst Fig. 6Aii and Aiii show similar records for S631A–HERG and N588K–HERG, respectively. In contrast to WT–HERG, for both S631A–HERG and N588K–HERG the $I_{HERG}$ tail magnitude was substantially smaller than the maximal current during the voltage-command (Fig. 6Aii and Aiii, respectively) reflecting the greatly attenuated $I_{HERG}$ inactivation of these HERG mutants [26,35,37]. Both mutant channels retained the ability to be inhibited by doxepin. Exponential fits to currents activated on depolarization to +20 mV for both mutants showed similar time-courses of current activation in control solution and following equilibration with 10 μM doxepin (S631A control: 60.6 ± 5.5 ms; doxepin: 64.5 ± 8.0 ms, $p > 0.5$; N588K control: 49.8 ± 6.2; doxepin: 41.7 ± 9.9 ms, $p > 0.5$; $n$ = 5 for both). Three

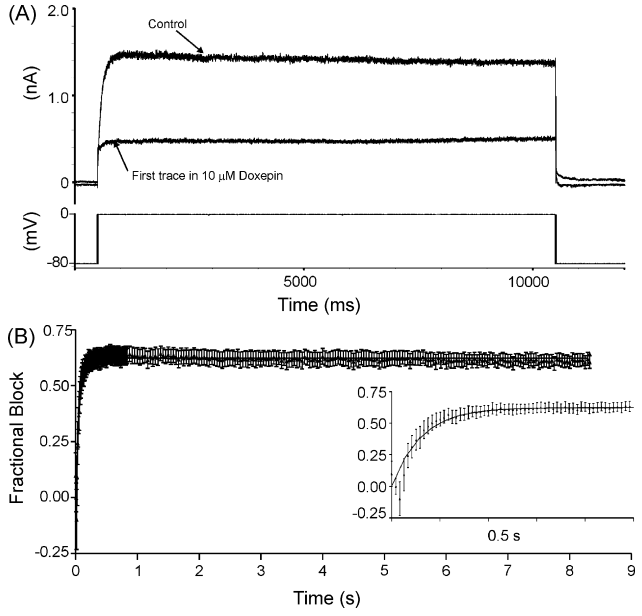


**Fig. 4 – Time-dependence of development of $I_{HERG}$ inhibition during a sustained depolarization. (A) Lower trace shows voltage-protocol (10 s depolarizing step from −80 to 0 mV) used to elicit $I_{HERG}$ in the absence of doxepin and following a 7-min exposure to 10 μM doxepin in the absence of pulsing. (B) Mean fractional block of $I_{HERG}$ ($n$ = 8) produced by 10 μM doxepin during the 10-s depolarizing step to 0 mV, following 7-min of drug application in the absence of pulsing. Inset shows, on an expanded time-scale, the development of blockade over the first 500 ms of the protocol. Monoexponential fitting of the fractional block time relationship yielded a rate constant (K) for the fit of 16.33 ± 0.73 $s^{-1}$ (equivalent to a time-constant (1/K) of 61 ms).**

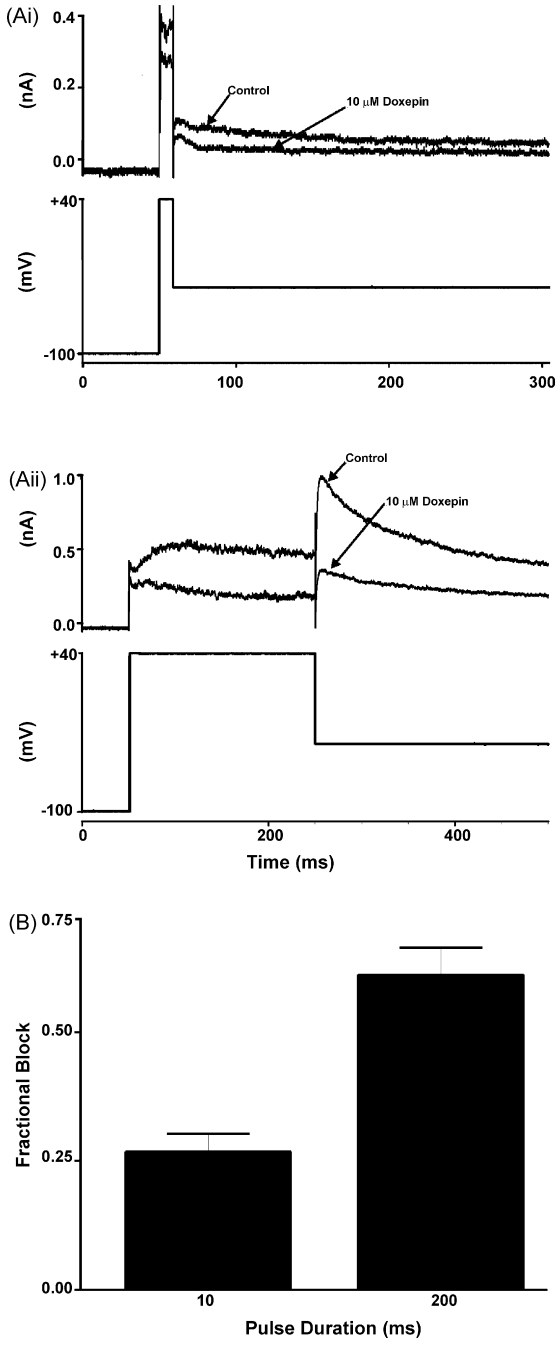


**Fig. 5 – $I_{HERG}$ inhibition by doxepin with brief-duration voltage-commands. (A) For each of (Ai) and (Aii), the upper traces show $I_{HERG}$ elicited by the voltage protocol shown in the lower trace: (Ai) shows representative traces of currents elicited by a 10-ms duration voltage command from −100 to +40 mV in the absence and presence of 10 μM doxepin; (Aii) shows data from the same cell with a 200 ms duration command. (B) Plot of mean (±S.E.M.) fractional block of $I_{HERG}$ tails following the 2 different duration commands ($n$ = 5; $p < 0.02$).**

doxepin concentrations (1, 10 and 100 μM) were tested to obtain concentration-response data. Fig. 6B shows concentration-response relations (determined using Eq. (2)) for $I_{HERG}$ tail inhibition for both S631A–HERG and N588K–HERG, with corresponding data for WT–HERG plotted for comparison. Although the S631A and N588K mutations produced small and modest increases, respectively, in the $IC_{50}$ derived from the fits to the concentration-response relations (from 6.6 μM for WT to 8.6 μM for S631A–HERG and 12.6 μM for N588K–HERG), these differences did not attain statistical significance ($p > 0.05$; Anova). These observations indicate the $I_{HERG}$ blockade by doxepin was not highly sensitive to attenuation of HERG channel inactivation.

### 3.5. *Sensitivity of $I_{HERG}$ inhibition by doxepin to the S6 mutations Y652A and F656A*

Two aromatic amino-acid residues, Y652 and F656, have been shown to be important components of the drug-binding site for a variety of HERG channel blockers [5,9,38]. Accordingly, we investigated whether or not doxepin inhibition of $I_{HERG}$ was sensitive to mutation of either residue, adopting a similar approach and protocols to those used in other recent $I_{HERG}$ pharmacology studies [29,32,39–41]. Fig. 7 shows the effects on doxepin inhibition of $I_{HERG}$ of the mutation Y652A (tyrosine → alanine). The experimental voltage protocol used (Fig. 7Aiii) was identical to that used for WT $I_{HERG}$ in Fig. 1

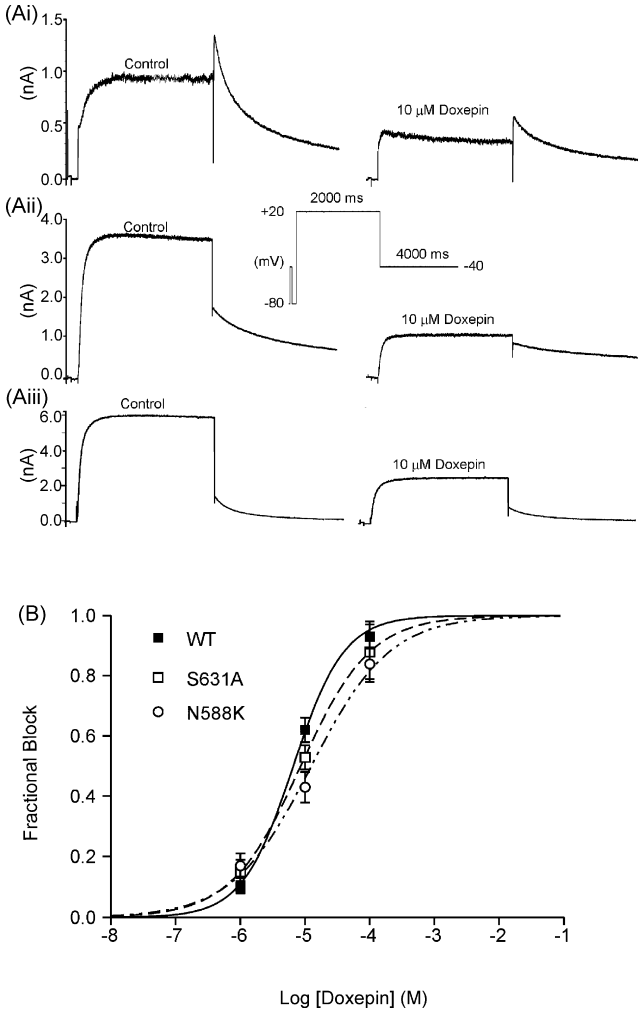


**Fig. 6 – (A) Effect of inactivation mutants on $I_{HERG}$ inhibition by doxepin. (Ai) Representative WT-HERG. (Aii) S631A-HERG and (Aiii) N588K-HERG currents in the absence (control, left hand traces) and presence of 10 μM doxepin (right hand traces). The voltage protocol is shown as an inset. (B). Mean fraction block of $I_{HERG}$ by 1, 10 and 100 μM doxepin (each drug concentration was applied to at least five cells; data for WT $I_{HERG}$ replotted from Fig. 1) fitted with Eq. (2). The derived $IC_{50}$ values for WT $I_{HERG}$, S631A–HERG and N588K–HERG were, respectively, 6.6 ± 0.6, 8.6 ± 0.0 and 12.6 ± 2.7 μM ($p > 0.05$; Anova); Hill coefficients for the fits to WT, S631A and N588K data were, respectively, 1.1 ± 0.1, 0.8 ± 0.0, and 0.7 ± 0.l ($p < 0.05$ between WT and N588K).**

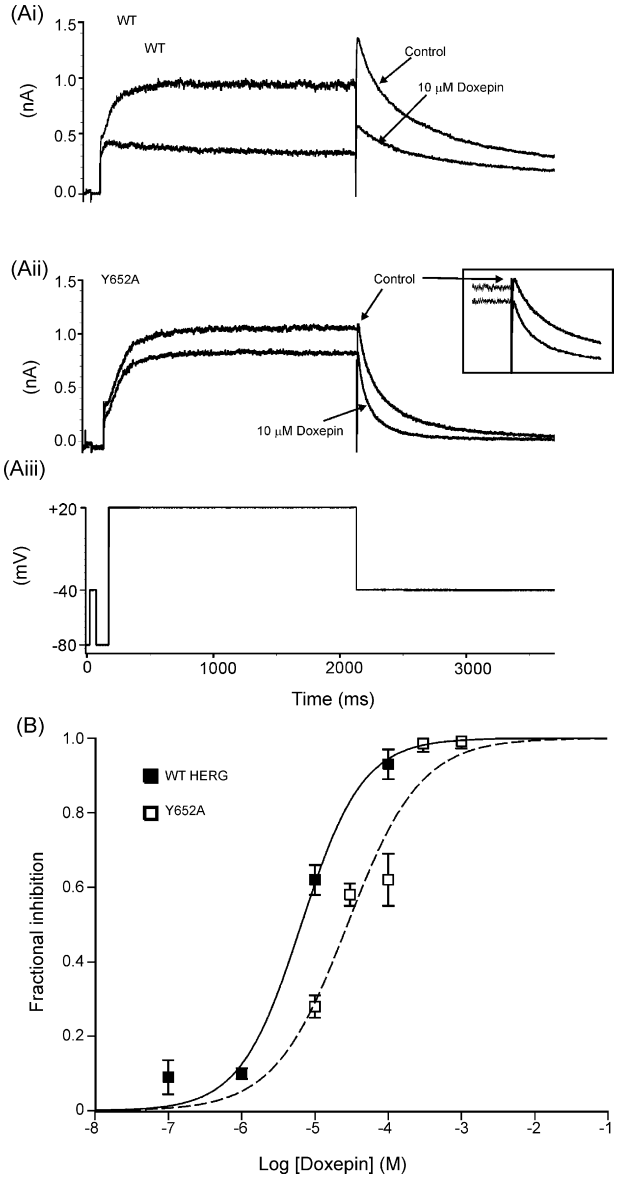


**Fig. 7 – (A) Effect of the Y652A mutation on $I_{HERG}$ inhibition by doxepin. (Ai) Representative WT-HERG and (Aii) Y652A-HERG currents in the absence and (Aiii) the presence of 10 μM doxepin, elicited by voltage protocol. Inset in (Aii) shows expanded tail-currents to highlight attenuation of blockade for the Y652A mutant.(B) Concentration-response relations for inhibition of $I_{HERG}$ by doxepin for WT–HERG and Y652A–HERG, fitted with Eq. (2). Data for WT $I_{HERG}$ are replotted from Fig. 1. For Y652A–HERG the following concentrations were tested: 10 μM ($n = 4$), 30 μM ($n = 4$); 100 μM ($n = 12$); 300 μM ($n = 4$) and 1 mM ($n = 4$). The derived $IC_{50}$ values for WT $I_{HERG}$ and Y652A $I_{HERG}$ were, respectively, 6.5 ± 1.4 and 27.8 ± 8.8 μM ($p < 0.05$); Hill coefficients for the fits to WT $I_{HERG}$ and Y652A $I_{HERG}$ of 1.0 ± 0.2 and 0.9 ± 0.3 ($p > 0.05$).**

and to investigate the S631A and N588K mutants in Fig. 6. Representative traces showing the effect of 10 μM doxepin on WT $I_{HERG}$ and Y652A $I_{HERG}$ are shown in Fig. 7Ai and Aii. WT $I_{HERG}$ was inhibited substantially by this doxepin concentration (Fig. 7Ai). In contrast, inhibition of Y652A $I_{HERG}$ was noticeably reduced (Fig. 7Aii; 28 ± 3% peak tail current inhibition compared to 62 ± 4% for WT $I_{HERG}$; $p < 0.001$). Four other doxepin concentrations (30, 100, 300μM and 1 mM) were also tested in order to construct a concentration response relation for inhibition of Y652A $I_{HERG}$ tails (Fig. 7B). A fit to the data with Eq. (2) (dashed line) yielded an $IC_{50}$ for inhibition of Y652A $I_{HERG}$ of 27.8 ± 8.8 μM (with a Hill coefficient of 0.9 ± 0.3), which represented a modest, though significant ($p < 0.05$), ~4.2 fold increase in $IC_{50}$ over that for WT $I_{HERG}$.

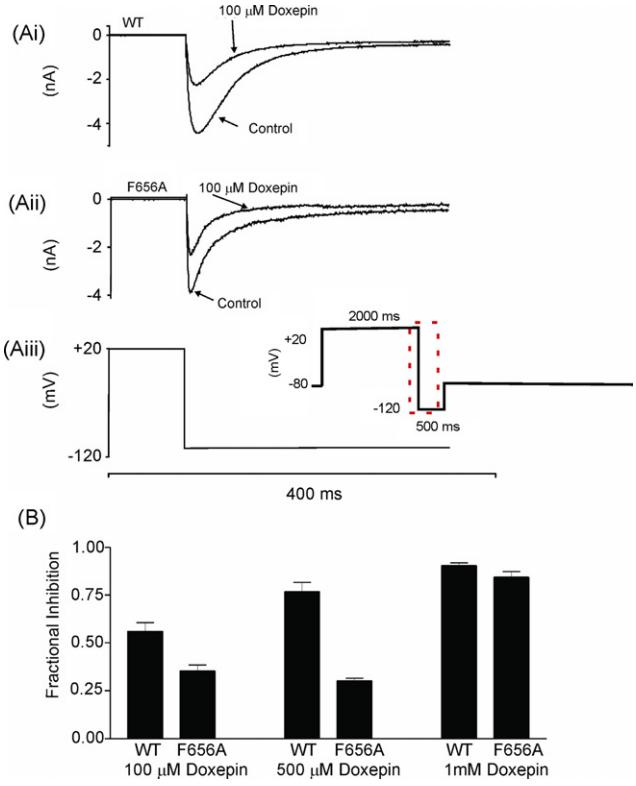


**Fig. 8 – (A) Effect of the F656A mutation on $I_{HERG}$ inhibition by doxepin. (Ai) Representative WT–HERG and (Aii) F656A-HERG currents in the absence and presence of 100 μM doxepin, elicited by voltage protocol (Aiii) on an expanded time-scale (full protocol shown as an inset). (B) Bar chart showing the mean fractional block levels produced for WT–HERG and F656A–HERG tails measured at −120 mV after addition of 100, 500 μM or 1 mM doxepin ($n = 5$ for each). The F656A mutation significantly attenuated the level of blockade produced by both 100 μM doxepin ($p < 0.01$) and 500 μM doxepin ($p << 0.001$), but not that by 1 mM doxepin ($p > 0.05$).**

$I_{HERG}$ carried by F656A–HERG channels was studied using the protocol shown in the inset of Fig. 8Aiii and inward tails were measured at −120 mV [25,28,29]. Initial experiments employed a doxepin concentration of 100 μM (shown in Fig. 1 to produce extensive inhibition of WT $I_{HERG}$ with a standard $[K^+]_e$). Representative traces showing effects of this concentration on WT and F656A $I_{HERG}$ are shown in Fig. 8Ai and Aii. The F656A mutation produced a modest attenuation of $I_{HERG}$ inhibition by this concentration of doxepin. However, as observed previously for some other drugs (e.g. [28]), the extent of inhibition of WT $I_{HERG}$ by 100 μM doxepin under conditions of high $[K^+]_e$ (see Section 2) was significantly smaller (56 ± 5%) than that observed with the same concentration in the experiments with a standard $[K^+]_e$ in Fig. 1 (93 ± 4%; $p < 0.001$). Therefore, the effects of two further concentrations of doxepin (500 μM and 1 mM) were also examined. Fig. 8B shows bar-chart plots of the mean levels of inhibition of WT and F656A $I_{HERG}$ by the three doxepin concentrations. These concentrations resulted in progressive increases in the level of blockade of WT $I_{HERG}$. In contrast, although Anova comparison of the data with the three drug concentrations confirmed that doxepin inhibition of F656A $I_{HERG}$ was concentration-dependent ($p < 0.001$), the observed concentration-dependence was unusual: there was no statistically significant difference between the observed level of blockade of F656A $I_{HERG}$ between 100 and 500 μM, whilst at 1 mM the observed level of inhibition of F656A $I_{HERG}$ was markedly increased ($p < 0.001$ compared to each of 100 and 500 μM, Bonferroni post-test) and approached that of WT $I_{HERG}$. Taken together, the data with the three doxepin concentrations suggest that the F656A mutation exerted some influence on the ability of doxepin to inhibit $I_{HERG}$, though the F656A data did not appear to follow a conventional monotonic concentration dependence.

## 4. Discussion

Despite a strong association between TCA use and QT interval lengthening [42], and although doxepin itself has been linked with both QT interval prolongation and TdP [18–20], the effects of this drug on HERG $K^+$ channels have not hitherto been reported. Moreover, whilst $I_{HERG}$ blockade has been investigated previously for the TCAs imipramine and amitriptyline [21–23], to our best knowledge the present study is the first in which molecular determinants of $I_{HERG}$ inhibition have been investigated for any member of the TCA family.

### 4.1. *Characteristics of $I_{HERG}$ blockade by doxepin*

Previously, imipramine has been reported to inhibit $I_{HERG}$ recorded in experiments using a mammalian expression system with an $IC_{50}$ of 3.4 μM [23] whilst an $IC_{50}$ of 10 μM was reported for amitriptyline [21]. A different study of amitriptyline, using the *Xenopus* oocyte expression system, reported $IC_{50}$'s of ~3.3–4.8 μM (depending on $[K^+]_e$) [22]. Thus, the potency of doxepin as an $I_{HERG}$ inhibitor found here ($IC_{50}$ of 6.5 μM) is broadly comparable to that seen previously for these other two TCAs. However, in terms of the characteristics of observed $I_{HERG}$ blockade, doxepin appears to be closer to imipramine than to amitriptyline: amitriptyline block of $I_{HERG}$ has been reported to show significant voltage-dependence [22] whereas imipramine showed only weak voltage-dependence [23]. Moreover, no significant effects of doxepin on the voltage-dependence of activation or inactivation were seen in this study. Unfortunately, comparative data for the TCAs imipramine and amitriptyline are lacking [21–23] and, therefore, a direct comparison between doxepin and these agents cannot be made in this regard. However, the atypical tetracyclic antidepressant maprotiline has recently been reported to show no alteration to the voltage-dependence of activation and inactivation [43], though another study contradicted this with regard to activation [44]. The lack of a significant leftward shift in the voltage-dependence of inactivation with doxepin in our study suggests that this agent does not act to stabilise $I_{HERG}$ inactivation, and the time-course of WT $I_{HERG}$ inactivation was not significantly accelerated by the drug. Moreover, the results with inactivation-attenuating mutations to two residues from distinct parts of the channel (S631A: outer mouth of the channel pore; N588K: in the S5-Pore linker) provide evidence that $I_{HERG}$ inactivation does not play an

obligatory role in doxepin's binding to the channel. This is further supported by unaltered levels of WT $I_{HERG}$ blockade with progressive depolarization over voltages at which $I_{HERG}$ was maximally activated, but over which inactivation increased (Fig. 3C and D). Doxepin is quite distinct in this regard from a number of other drugs, including the archetypal high affinity HERG blocking methanesulphonanilide drugs E-4031 and dofetilide, for which $I_{HERG}$ inactivation exerts a strong influence on blocking potency – either as a direct consequence of inactivation-state dependent block, or due to conformational changes during inactivation facilitating optimal orientation of S6 helical residues to which drugs bind [10,45–48].

Blockade of $I_{HERG}$ by imipramine has been reported to develop rapidly during a sustained depolarization, with a component of inhibition visible even for comparatively brief depolarizing voltage commands [23]. These features of imipramine's action correspond well with those seen for doxepin in the present study. They are also similar to those reported for the serotonin-selective reuptake inhibitors (SSRIs) fluvoxamine and citalopram [25,49], but differ significantly from the methanesulphonanilides, for which little blockade is observed immediately upon depolarization, with blockade then increasing progressively during the maintained depolarization [24,49,50]. The lack of a strong dependence of HERG channel blockade by doxepin on $I_{HERG}$ inactivation suggests that gating-dependent blockade by this drug is likely to arise predominantly to activated/open channels. Accordingly, the observed time-dependence of $I_{HERG}$ inhibition by doxepin in this study is consistent with either a mixed state-dependence of blockade (with components of both closed and open channel blockade) or with the presence of a very rapidly developing component of activation-dependent inhibition immediately on depolarization.

For the majority of drugs that have been studied, one or both of the Y652 and F656 aromatic amino acid residues in the S6 helices of the HERG channel comprise key elements of the drug binding site [5,9,38,51]. For example, the Y652A and F656A mutations increased the $IC_{50}$ for HERG blockade by the methanesulphonanilide MK-499 by 94-fold and 650-fold, respectively, and that for terfenadine by ~100-fold [8]. In comparison, the ~4-fold increase in $IC_{50}$ for doxepin produced by the Y652A mutation in this study, is rather modest, suggesting that this residue is less influential for binding of doxepin than for either of these high affinity blockers. The unusual concentration dependence seen with the F656A mutation indicated that at a high doxepin concentration of 1 mM $I_{HERG}$ blockade was little affected by mutation of this residue, whilst at concentrations of 100 and 500 μM significant attenuation of blockade occurred with no significant increase in block at 500 μM compared to 100 μM. It was not possible to obtain an adequate fit of these data with Eq. (2). A cautious interpretation of the lack of a conventional concentration-dependence of F656A–HERG inhibition by doxepin is that blockade may depend partly, but incompletely, on this residue. Neither the Y652A nor F656A mutations attenuated blockade by doxepin concentrations producing very high levels (>90%) of blockade of WT $I_{HERG}$, suggesting that neither residue is absolutely obligatory for doxepin binding to HERG channels to occur. Whilst unusual, this is not unprecedented; $I_{HERG}$ block by both the SSRI fluvoxamine and the antiarrhythmic agent dronedarone has been reported to be only partially attenuated by the Y652A and F656A mutations [25,28]. Comparative data for other TCAs are lacking, though recently these residues have been implicated in $I_{HERG}$ inhibition by the tetracyclic drug maprotiline [43,44]; one of these two studies obtained $IC_{50}$ values for the Y652A and F656T mutants, with respective (modest) 3-fold and 7-fold increases in $IC_{50}$ [43]. Whilst obligatory molecular determinants of doxepin-binding to HERG remain to be found, the fact that $I_{HERG}$ inhibition by doxepin developed progressively over several minutes following rapid external solution exchange is consistent with the drug crossing the cell membrane to reach its site of action. The reduced $I_{HERG}$ inhibition by doxepin of WT $I_{HERG}$ in the presence of raised $[K^+]_e$ may also be of significance. Since $I_{HERG}$ inhibition by doxepin appears not to be critically dependent on channel inactivation, decreased blockade with high $[K^+]_e$ is unlikely to result from any effect of $[K^+]_e$ on $I_{HERG}$ inactivation. Rather, reduced inhibition in high $[K^+]_e$ may be accounted for by an interference with drug-binding due to an electrostatic repulsion or ''knock-off'' process [28,52], consistent with drug binding to the channel at a site close to the ion conduction pathway. It remains to be determined whether this site would need to reside within the channel pore. However, in a limited series of experiments using the D540K mutant [53], we did not find evidence that doxepin can readily unbind on hyperpolarization-induced channel opening (data not shown); though not all drugs that bind within the pore exhibit marked 'untrapping' [54]. Nevertheless, given the presence of a significant component of $I_{HERG}$ blockade with brief depolarization and incomplete attenuation of inhibition by the Y652A and F656A mutations, we cannot exclude the possibilities that a proportion of the observed blockade with doxepin involves binding outside of the channel pore, or binding to closed HERG channels.

### 4.2. *Clinical significance of $I_{HERG}$ blockade by doxepin*

TCAs are associated with $QT_c$ interval lengthening in clinical use [42], and $I_{HERG}$ inhibition by doxepin observed in the present study is consistent both with documented cases of QT interval prolongation and TdP with doxepin [18–20] and with QT interval increases seen in anaesthetised guinea-pigs receiving doxepin infusion [15]. Our study was conducted at a physiologically relevant temperature and the extent of $I_{HERG}$ blockade by doxepin was similar between ventricular action potential and conventional voltage step protocols. A lack of relief of $I_{HERG}$ blockade on membrane hyperpolarization for the D540K mutant (mentioned in Section 4.1, above) is suggestive of relatively poor drug unbinding at negative voltages in the maintained presence of drug, whilst the data shown in Fig. 5 indicate that at 10 μM (the same concentration as used for the AP clamp experiment in Fig. 2) doxepin was able to bind and inhibit $I_{HERG}$ rapidly on membrane depolarization to a positive voltage. These factors may combine to account for the similar levels of $I_{HERG}$ inhibition by doxepin observed with step and AP clamp protocols. Although we did not co-express HERG with MiRP1, a putative $\beta$ subunit suggested to be necessary to recapitulate native $I_{Kr}$ [55], it has recently been suggested that

MiRP1 is unlikely to interact with HERG outside of the cardiac conduction system [51] and, additionally, the pharmacological sensitivity of HERG channels expressed in mammalian cells without MiRP1 co-expression has been found to be similar to that of native $I_{Kr}$ [56]. This notion is reinforced by the close concordance of inhibitory potency of doxepin on $I_{HERG}$ and native $I_{Kr}$ in our experiments ($IC_{50}$ values of 6.5 and 4.4 μM, respectively). A question therefore arises as to the relationship between the potency of $I_{HERG}/I_{Kr}$ blockade seen in this study and plasma concentrations of doxepin in patients. As a class, the TCAs are lipophilic and are known to become concentrated in some tissues, including the myocardium [57]. In the case of doxepin, one experimental study has reported doxepin concentration in cardiac muscle to be 41-fold higher than plasma levels [58]. This makes it difficult to extrapolate with accuracy from known plasma concentrations to likely levels of $I_{HERG}/I_{Kr}$ blockade by doxepin in vivo. The therapeutic plasma level of doxepin is thought to be between 50 and 250 ng/ml (0.16–0.8 μM), although a wide variety of recommendations from university psychiatric departments and laboratories (up to 1000 ng/ml; 3.2 μM) have been reported [59]. Whilst $I_{HERG}$ (or $I_{Kr}$) blockade at the lower end of this range might be anticipated to be modest, inhibition at higher concentrations would be significant and, taking into account also potential cardiac accumulation, the observed potency of $I_{HERG}$ inhibition by doxepin in this study is likely to be clinically relevant, particularly in overdose. Such an effect may be exacerbated in individuals exhibiting pre-existing QT interval prolongation (congenital or acquired), electrolyte abnormalities or with impaired drug metabolism. Thus, as for other $I_{HERG}$ blocking medications, caution is warranted in its use in patients with pre-existing QT interval prolongation or with risk factors likely to exacerbate the effects of $I_{HERG}$ blocking medications.

The findings of this study have further clinical relevance in a second, perhaps less expected, respect. The attenuated-inactivation N588K–HERG mutant used in this study has been shown recently to underlie the SQT1 familial form of the recently identified genetic 'Short QT syndrome', which carries a risk of cardiac arrhythmia and sudden death [27,60]. Pharmacological approaches to correcting the QT-interval of SQT1 patients are currently very limited. These patients are comparatively insensitive to Class III $I_{Kr}$/HERG blocking drugs [27,61] and the N588K–HERG blocking potencies of the $I_{Kr}$/HERG blockers E-4031and D-sotalol are reduced ~12–20-fold compared to their effects on WT–HERG [62,63], presumably due to a role (direct or otherwise) of channel inactivation in facilitating drug binding to the HERG channel. To date, only the Class *Ia* antiarrhythmic drug quinidine has been found both to inhibit N588K–HERG effectively and to correct the QT interval in such patients [27,62,63]; however, very recently, another Class *Ia* antiarrhythmic, disopyramide, has been shown to be effective against N588K–HERG in vitro [63]. The present study identifies doxepin as both an $I_{HERG}$-blocker for which channel inactivation does not play a major role in drug binding and as an additional drug that is an effective inhibitor of N588K–HERG. Whilst the sedative effects of doxepin may make it unsuitable as a corrective treatment for SQT1 patients, our findings prompt the question as to whether chemical structures related to doxepin might feasibly offer viable $I_{HERG}$ blocking agents in SQT1.

## Acknowledgements

RSD was funded by a BBSRC/Pfizer 'CASE' studentship. The authors also acknowledge support from the British Heart Foundation (PG/03/121, PG/04/090, PG/06/139) and thank Mrs Lesley Arberry for technical assistance.

## REFERENCES

[1] Viskin S. Long QT syndromes and torsade de pointes. Lancet 1999;354:1625–33.
[2] Haverkamp W, Breithardt G, Camm AJ, Janse MJ, Rosen MR, Antzelevitch C, et al. The potential for QT prolongation and pro-arrhythmia by non-anti-arrhythmic drugs: clinical and regulatory implications report on a policy conference of the European Society of Cardiology.. Cardiovasc Res 2000;47: 219–33.
[3] Shah RR. Drugs QT interval prolongation and ICH E14—the need to get it right. Drug Safety 2005;28:115–25.
[4] Witchel HJ, Hancox JC. Familial and acquired long QT syndrome and the cardiac rapid delayed rectifier potassium current. Clin Exp Pharmacol Physiol 2000;27: 753–66.
[5] Vandenberg JI, Walker BD, Campbell TJ. HERG $K^+$ channels: friend and foe. Trends Pharmacol Sci 2001;22:240–6.
[6] Sanguinetti MC, Jiang C, Curran ME, Keating MT. A mechanistic link between an inherited and an acquired cardiac arrhythmia: HERG encodes the $I_{Kr}$ potassium channel. Cell 1995;81:299–307.
[7] Trudeau MC, Warmke JW, Ganetzky B, Robertson GA. HERG a human inward rectifier in the voltage-gated potassium channel family. Science 1995;269:92–5.
[8] Mitcheson JS, Chen J, Lin M, Culberson C, Sanguinetti MC. A structural basis for drug-induced long QT syndrome. Proc Natl Acad Sci USA 2000;97:12329–33.
[9] Mitcheson JS, Perry MD. Molecular determinants of high-affinity drug binding to HERG channels. Curr Opin Drug Discov Devel 2003;6:667–74.
[10] Lees-Miller JP, Duan YJ, Teng GQ, Duff HJ. Molecular determinant of high-affinity dofetilide binding to HERG1 expressed in Xenopus oocytes: Involvement of S6 sites. Mol Pharmacol 2000;57:367–74.
[11] Webster R, Leishman D, Walker D. Towards a drug concentration effect relationship for QT prolongation and torsades de pointes. Curr Opin Drug Discov Devel 2002;5:116–26.
[12] Bridgland-Taylor MH, Hargreaves AC, Easter A, Orme A, Henthorn DC, Ding M, et al. Optimisation and validation of a medium-throughput electrophysiology-based hERG assay using IonWorks(TM) HT. J Pharmacol Toxicol Meth 2006;54:189–99.
[13] Redfern WS, Carlsson L, Davis AS, Lynch WG, MacKenzie I, Palethorpe S, et al. Relationships between preclinical cardiac electrophysiology, clinical QT interval prolongation and torsade de pointes for a broad range of drugs: evidence for a provisional safety margin in drug development. Cardiovasc Res 2003;58:32–45.
[14] Pinder RM, Brogden RN, Speight TM, Avery GS, Doxepin Up-To-Date. Review of its pharmacological properties and therapeutic efficacy with particular reference to depression. Drugs 1977;13:161–218.
[15] Dumovic P, Burrows GD, Vohra J, Davies B, Scoggins BA. The effect of tricyclic antidepressant drugs on the heart. Arch Toxicol 1976;35:255–62.
[16] Luchins DJ. Review of clinical and animal studies comparing the cardiovascular effects of doxepin and

other tricyclic antidepressants. Am J Psychiatry 1983;140:1006–9.
[17] Roose SP, Dalack GW, Glassman AH, Woodring S, Walsh BT, Giardina EG. Is doxepin a safer tricyclic for the heart? J Clin Psychiatry 1991;52:338–41.
[18] Baker B, Dorian P, Sandor P, Shapiro C, Schell C, Mitchell J, et al. Electrocardiographic effects of fluoxetine and doxepin in patients with major depressive disorder. J Clin Psychopharmacol 1997;17:15–21.
[19] Alter P, Tontsch D, Grimm W. Doxepin-induced torsade de pointes tachycardia. Ann Intern Med 2001;135:384–5.
[20] Rademacher S, Dietz R, Haverkamp W. QT prolongation and syncope with methadone, doxepin, and a beta-blocker. Ann Pharmacother 2005;39:1762–3.
[21] Tie H, Walker BD, Valenzuela SM, Breit SN, Campbell TJ. The heart of psychotropic drug therapy. Lancet 2000;355:1825–11825.
[22] Jo SH, Youm JB, Lee CO, Earm YE, Ho WK. Blockade of the HERG human cardiac $K^+$ channel by the antidepressant drug amitriptyline. Br J Pharmacol 2000;129:1474–80.
[23] Teschemacher AG, Seward EP, Hancox JC, Witchel HJ. Inhibition of the current of heterologously expressed HERG potassium channels by imipramine and amitriptyline. Br J Pharmacol 1999;128:479–85.
[24] Zhou Z, Gong Q, Ye B, Fan Z, Makielski JC, Robertson GA, et al. Properties of HERG channels stably expressed in HEK 293 cells studied at physiological temperature. Biophys J 1998;74:230–41.
[25] Milnes JT, Crociani O, Arcangeli A, Hancox JC, Witchel HJ. Blockade of HERG potassium currents by fluvoxamine: incomplete attenuation by S6 mutations at F656 or Y652. Br J Pharmacol 2003;139:887–98.
[26] Zou A, Xu QP, Sanguinetti MC. A mutation in the pore region of HERG $K^+$ channels expressed in Xenopus oocytes reduces rectification by shifting the voltage dependence of inactivation. J Physiol 1998;509:129–37.
[27] Brugada R, Hong K, Dumaine R, Cordeiro J, Gaita F, Borggrefe M, et al. Sudden death associated with short-QT syndrome linked to mutations in HERG. Circulation 2004;109:30–5.
[28] Ridley JM, Milnes JT, Witchel HJ, Hancox JC. High affinity HERG $K^+$ channel blockade by the antiarrhythmic agent dronedarone: resistance to mutations of the S6 residues Y652 and F656. Biochem Biophys Res Commun 2004;325:883–91.
[29] Duncan RS, Ridley JM, Dempsey CE, Leishman DJ, Leaney JL, Hancox JC, et al. Erythromycin block of the HERG $K^+$ channel: accessibility to F656 and Y652. Biochem Biophys Res Commun 2006;341:500–6.
[30] Hancox JC, Levi AJ, Lee CO, Heap P. A method for isolating rabbit atrioventricular node myocytes which retain normal morphology and function. Am J Physiol 1993;265:H755–666.
[31] Howarth FC, Levi AJ, Hancox JC. Characteristics of the delayed rectifier K current compared in myocytes isolated from the atrioventricular node and ventricle of the rabbit heart. Pflugers Arch 1996;431:713–22.
[32] Ridley JM, Milnes JT, Hancox JC, Witchel HJ, Clemastine. A conventional antihistamine, is a high potency inhibitor of the HERG $K^+$ channel. J Mol Cell Cardiol 2006;40:107–18.
[33] Kirsch GE, Trepakova ES, Brimecombe JC, Sidach SS, Erickson HD, Kochan MC, et al. Variability in the measurement of hERG potassium channel inhibition: effects of temperature and stimulus pattern. J Pharmacol Toxicol Meth 2004;50:93–101.
[34] Ridley JM, Milnes JT, Zhang YH, Witchel HJ, Hancox JC. Inhibition of HERG $K^+$ current and prolongation of the guinea-pig ventricular action potential by 4-aminopyridine. J Physiol 2003;549:667–72.
[35] McPate MJ, Duncan RS, Milnes JT, Witchel HJ, Hancox JC. The N588K-HERG $K^+$ channel mutation in the 'short QT syndrome': mechanism of gain-in-function determined at 37 °C. Biochem Biophys Res Commun 2005;334:441–9.
[36] Milnes JT, Dempsey CE, Ridley JM, Crociani O, Arcangeli A, Hancox JC, et al. Preferential closed channel blockade of HERG potassium currents by chemically synthesised BeKm-1 scorpion toxin. FEBS Lett 2003;547:20–6.
[37] Cordeiro JM, Brugada R, Wu YS, Hong K, Dumaine R. Modulation of $I_{Kr}$ inactivation by mutation N588K in KCNH2: a link to arrhythmogenesis in short QT syndrome. Cardiovasc Res 2005;67:498–509.
[38] Sanguinetti MC, Mitcheson JS. Predicting drug-HERG channel interactions that cause acquired long QT syndrome. Trends Pharmacol Sci 2005;26:119–24.
[39] Ridley JM, Dooley PC, Milnes JT, Witchel HJ, Hancox JC. Lidoflazine is a high affinity blocker of the HERG $K^+$ channel. J Mol Cell Cardiol 2004;36:701–5.
[40] Alexandrou AJ, Duncan RS, Sullivan A, Hancox JC, Leishman DJ, Witchel HJ, et al. Mechanism of hERG $K^+$ channel blockade by the fluoroquinolone antibiotic moxifloxacin. Br J Pharmacol 2006;147:905–16.
[41] Ridley JM, Milnes JT, Duncan RS, McPate MJ, James AF, Witchel HJ, et al. Inhibition of the HERG $K^+$ channel by the antifungal drug ketoconazole depends on channel gating and involves the S6 residue F656. FEBS Lett 2006;580:1999–2005.
[42] Reilly JG, Ayis SA, Ferrier IN, Jones SJ, Thomas SHL. QTc-interval abnormalities and psychotropic drug therapy in psychiatric patients. Lancet 2000;355:1048–52.
[43] Kiesecker C, Alter M, Kathofer S, Zitron E, Scholz E, Thomas PD, et al. Atypical tetracyclic antidepressant maprotiline is an antagonist at cardiac hERG potassium channels. Naunyn-Schmiedebergs Arch Pharmacol 2006;373:212–20.
[44] Ferrer-Villada T, Navarro-Polanco RA, Rodriguez-Menchaca AA, Benavides-Haro DE, Sanchez-Chapula JA. Inhibition of cardiac HERG potassium channels by antidepressant maprotiline. Eur J Pharmacol 2006;531:1–8.
[45] Ficker E, Jarolimek W, Kiehn J, Baumann A, Brown AM. Molecular determinants of dofetilide block of HERG $K^+$ channels. Circ Res 1998;82:386–95.
[46] Herzberg IM, Trudeau MC, Robertson GA. Transfer of rapid inactivation and sensitivity to the class III antiarrhythmic drug E-4031 from HERG to M-eag channels. J Physiol 1998;511:3–14.
[47] Yang BF, Xu DH, Xu CQ, Li Z, Du ZM, Wang HZ, et al. Inactivation gating determines drug potency: a common mechanism for drug blockade of HERG channels. Acta Pharmacologica Sinica 2004;25:554–60.
[48] Chen J, Seebohm G, Sanguinetti MC. Position of aromatic residues in the S6 domain, not inactivation, dictates cisapride sensitivity of HERG and eag potassium channels. Proc Nat Acad Sci USA 2002;99:12461–6.
[49] Witchel HJ, Pabbathi VK, Hofmann G, Paul AA, Hancox JC. Inhibitory actions of the selective serotonin re-uptake inhibitor citalopram on HERG and ventricular L-type calcium currents. FEBS Lett 2002;512:59–66.
[50] Snyders DJ, Chaudhary A. High affinity open channel block by dofetilide of HERG expressed in a human cell line. Mol Pharmacol 1996;49:949–55.
[51] Sanguinetti MC, Tristan-Firouzi M. HERG potassium channels and cardiac arrhythmia. Nature 2006;440:463–9.
[52] Wang S, Morales MJ, Liu S, Strauss HC, Rasmusson RL. Modulation of HERG affinity for E-4031 by $[K^+]_o$ and C-type inactivation. FEBS Lett 1997;417:43–7.
[53] Mitcheson JS, Chen J, Sanguinetti MC. Trapping of a Methanesulfonanilide by closure of the HERG potassium channel activation gate. J Gen Physiol 2000;115:229–40.

[54] Perry M, de Groot MJ, Helliwell R, Leishman D, Tristani-Firouzi M, Sanguinetti MC, et al. Structural determinants of HERG channel block by clofilium and ibutilide. Mol Pharmacol 2004;66:240–9.
[55] Abbott GW, Sesti F, Splawski I, Buck ME, Lehmann WH, Timothy KW, et al. MiRP1 forms $I_{Kr}$ potassium channels with HERG and is associated with cardiac arrhythmia. Cell 1999;97:175–87.
[56] Weerapura M, Nattel S, Chartier D, Caballero R, Hebert TE. A comparison of currents carried by HERG, with and without coexpression of MiRP1, and the native rapid delayed rectifier current Is MiRP1 the missing link. J Physiol 2002;540:15–27.
[57] Marshall JB, Forker AD. Cardiovascular effects of tricyclic antidepressant drugs: therapeutic usage, overdose, and management of complications. Am Heart J 1982;103:401–14.
[58] Elonen E, Linnoila M, Lukkari I, Mattila MJ. Concentration of tricyclic antidepressants in plasma, heart and skeletal muscle after their intravenous infusion to anaesthetized rabbits. Acta Pharmacol Toxicol 1975;37:274–81 (Copenh).
[59] Leucht S, Steimer W, Kreuz S, Abraham D, Orsulak PJ, Kissling W. Doxepin plasma concentrations: is there really a therapeutic range? J Clin Psychopharmacol 2001;21:432–9.
[60] Brugada R, Hong K, Cordeiro JM, Dumaine R. Short QT Syndrome. CMAJ 2005;173:1349–54.
[61] Gaita F, Giustetto C, Bianchi F, Schimpf R, Haissaguerre M, Calo L, et al. Short QT syndrome: pharmacological treatment. J Am Coll Cardiol 2004;43:1494–9.
[62] Wolpert C, Schimpf R, Giustetto C, Antzelevitch C, Cordeiro J, Dumaine R, et al. Further insights into the effect of quinidine in short QT syndrome caused by a mutation in HERG. J Cardiovasc Electrophysiol 2005;16:54–8.
[63] McPate MJ, Duncan RS, Witchel HJ, Hancox JC. Disopyramide is an effective inhibitor of mutant HERG K+ channels involved in variant 1 short QT syndrome. J Mol Cell Cardiol 2006;41:563–6.